Design of Two-Channel Bilateral Control Systems by a Transfer-Function-Based Approach

Masahiro Tajiri , *Student Member, IEEE*, Pablo López, and Yasutaka Fujimoto , *Senior Member, IEEE*

Abstract—In this paper, we propose a design method of a two-channel bilateral control system using an approach based on transfer function. The configuration of such a control system can be realized by designing a complementary sensitivity function. Compared with the conventional four-channel bilateral control, our system has better control performance and requires fewer communication channels. The proposed scheme can be extended to micro/macro bilateral control that changes the scaling ratio of the master to slave systems. The proposed bilateral control can be realized simply by using a simple controller. In order to compare performances of the proposed method and the conventional four-channel bilateral control, ordinary bilateral control and micro/macro bilateral control are performed by a simple experimental machine with a one-degree-of-freedom mechanism. We discuss the features of each method by comparing the transparency and operability of both methods.

Index Terms—Bilateral control, haptics, micro/macro bilateral control, motion control, reproducibility and operability.

I. INTRODUCTION

IN RECENT years, haptic technology has attracted attention for transmission of human sensory information following transmission of visual and auditory senses [1]. Haptic communication has a bilateral information flow transmitting behaviors and their reaction, while the conventional visual and auditory communication require only a unilateral information flow. This important difference makes it difficult to realize haptic communication. Because real-time information is essential for bilateral communication, bilateral control can be considered as a means for realizing haptic transmission.

Bilateral control systems are divided into two or more subsystems. Each subsystem is equipped with actuators and sensors having one or more degrees of motion freedom. One side is

called the "master" side and the other is called the "slave side." The slave subsystem tracks the position of the master system as though it is mechanically connected, and the master side provides the operator with the force encountered by the slave side [2], [3].

Many researchers have investigated bilateral control that realizes haptic transmission [4], [5]. Many of their studies on bilateral control have demonstrated highly accurate haptic feedback from remote places. Bilateral control systems are often regarded as two-port models [6]. Lawrence proposed a performance indicator to evaluate the reproduction of remote environments [7], [8]. The control target in designing a bilateral control system is to achieve position and force synchronization between the master and the slave [9], [10]. It is pointed out that the control system cannot maintain transparency and stability at the same time because of the uncertainty that exists in the environment, and therefore, there is a tradeoff between these two goals [11], [12]. A system based on acceleration control has been reported as a bilateral control system based on a four-channel architecture. That system has demonstrated high transparency and maneuverability [13]–[15]. Since the position and force controls are unified through acceleration-based control, the position and force can be precisely controlled. The bilateral control method based on the four-channel architecture is currently the most studied haptic transmission method. Another method of achieving acceleration control is using a sliding mode controller [16]–[18]. In this method, when the structure of the master and the slave robots are different, the control precision is lowered. A method using a hybrid controller has been reported to deal with this problem [19].

However, four-channel controllers use various estimation systems such as a disturbance observer (DOB) to realize a very transparent system. Furthermore, the position and force controllers must be independently designed, and control is performed using two types of information, position and force. For these reasons, information that has to be transmitted increases, and a means of communication of haptic data has had to be studied [20], [21].

Therefore, control methods for further simplifying bilateral control methods based on the two-channel control system, thus reducing the information needed, are being studied [22], [23]. These studies have proposed a new method for designing a bilateral control system based on feedback of only position

information without using reaction force estimation. In such systems, the position and force response characteristics of the master/slave system are analyzed based on the transfer function of the system. By designing a complementary sensitivity function that determines the transfer function, they realized a bilateral control system considering transparency and stability. Thus, using a system with a small amount of information, they were successful in realizing a bilateral control system using only position information, without using a subsystem such as an estimator of the control system.

As an application example of haptic transmission technology, a highly sensitive bilateral teleoperation system can be applied to various industry fields such as rehabilitation, medical support robot, production industry, and entry into hazardous areas. In the rehabilitation field, a haptic training system has been introduced and efficient training is being studied [24]. In the medical field, a system that allows a doctor to operate, by bilateral control, a robot to perform endoscopic surgeries, thus reducing the burden on a patient, is expected [25]. Furthermore, in industry, mechanization of many more processes has been progressing by applying multilateral control and a motion copying system [26], [27] that extends the multiple master/slave system [28]–[30]. In order to achieve these goals, we need a scaling technology to apply bilateral control to master/slave robot systems of different sizes. Also, since these robots usually require several degrees of freedom, the control system should be more flexible. Therefore, many methods are being studied for realizing micro/macro bilateral control [31]–[33]. Since these methods are designed based on four-channel bilateral control, they cannot deal with the problems mentioned previously. In the proposed method in this paper, it is possible to introduce micro/macro bilateral control by introducing a scaling factor. The introduction of the scaling factor does not affect the stability and transparency of the system. Therefore, in this paper, we compare the performance of two-channel bilateral control and four-channel bilateral control. This comparison demonstrates the theoretical and experimental aspects of reproducibility and operability, which is a performance index of bilateral control. Furthermore, we introduce macro/micro bilateral control to two-channel bilateral control and discuss the applicability of the method. We confirm the effectiveness of two-channel bilateral control in this paper.

This paper is organized as follows. Section II describes the structure of the control system based on parametrization of the complementary sensitivity function. In Section III, we describe the design of an important Q parameter to determine the response and stability of the control system. An analysis of the reproducibility and usability of the proposed method is shown in Section IV. As a presentation of expandability, Section V describes implementation of bilateral control with a single controller and Section VI describes the design of micro/macro bilateral control. The experimental results for each method are shown in Section VII, and the final section summarizes this paper.

II. STRUCTURE OF THE PROPOSED BILATERAL CONTROL SYSTEM

Fig. 1 shows the basic structure of the proposed bilateral control system consisting of two communication channels and four
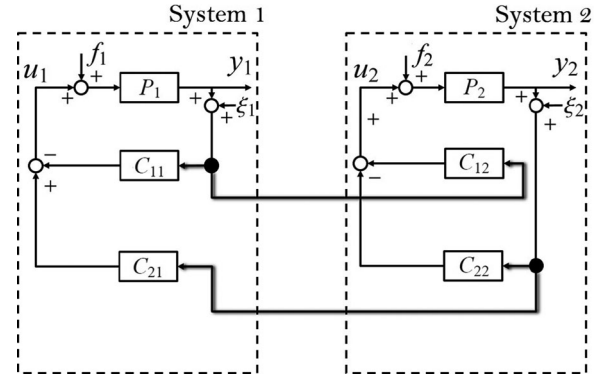

Fig. 1. Block diagram of the proposed bilateral control system.

feedback controllers. Variables in Fig. 1 represent the following: u_n means controller's output; P_n is the nominal plant model; C_n expresses the controller's function; and f_n and ξ_n are the external force and observation noise, respectively, as input signals. The four controllers are divided into two types: feedback controller for stabilization and controller for transmitting information to other systems. There are two controlled plants P_1 and P_2 driven by corresponding input u_1 and u_2 and external force f_1 and f_2. The goal of this control system is to realize the law of momentum conservation in terms of the external force, i.e., the law of action and reaction between the external forces applied to the controlled plants while their positions are synchronized. We consider MIMO feedback from two position observations of the motion system is the input to two actuators. A design of the control system can be derived by a transfer-function-based approach.

From Fig. 1, relations between the external force f, observation noise for encoder signal ξ, the position output of the controlled plant y, and the control input u are as follows:

$$y_1 = P_1(f_1 + u_1) \tag{1}$$

$$y_2 = P_2(f_2 + u_2) \tag{2}$$

$$u_1 = -C_{11}(y_1 + \xi_1) + C_{21}(y_2 + \xi_2) \tag{3}$$

$$u_2 = C_{12}(y_1 + \xi_1) - C_{22}(y_2 + \xi_2). \tag{4}$$

Equations (1)–(4) can be summarized as follows:

$$\begin{bmatrix} \boldsymbol{y}(s) \\ \boldsymbol{u}(s) \end{bmatrix} = \frac{1}{A} \begin{bmatrix} \boldsymbol{G}_{yf}(s) & \boldsymbol{G}_{y\xi}(s) \\ \boldsymbol{G}_{uf}(s) & \boldsymbol{G}_{u\xi}(s) \end{bmatrix} \begin{bmatrix} \boldsymbol{f}(s) \\ \boldsymbol{\xi}(s) \end{bmatrix} \tag{5}$$

where

$$\boldsymbol{y}(s) = \begin{bmatrix} y_1 \\ y_2 \end{bmatrix}, \quad \boldsymbol{u}(s) = \begin{bmatrix} u_1 \\ u_2 \end{bmatrix} \tag{6}$$

$$\boldsymbol{f}(s) = \begin{bmatrix} f_1 \\ f_2 \end{bmatrix}, \quad \boldsymbol{\xi}(s) = \begin{bmatrix} \xi_1 \\ \xi_2 \end{bmatrix} \tag{7}$$

$$\boldsymbol{G}_{yf}(s) = \begin{bmatrix} (1 + C_{22}P_2)P_1 & C_{21}P_1P_2 \\ C_{12}P_1P_2 & (1 + C_{11}P_1)P_2 \end{bmatrix} \tag{8}$$

$$\boldsymbol{G}_{y\xi}(s) = \begin{bmatrix} (1 + C_{22}P_2) - A & C_{21}P_1 \\ C_{12}P_2 & (1 + C_{11}P_1) - A \end{bmatrix} \quad (9)$$

$$\boldsymbol{G}_{uf}(s) = \begin{bmatrix} (1 + C_{22}P_2) - A & C_{21}P_2 \\ C_{12}P_1 & (1 + C_{11}P_1) - A \end{bmatrix} \quad (10)$$

$$\boldsymbol{G}_{u\xi}(s) = \begin{bmatrix} -C_{11} + P_2 B & C_{21} \\ C_{12} & -C_{22} + P_1 B \end{bmatrix} \quad (11)$$

$$A = (1 + C_{11}P_1)(1 + C_{22}P_2) - C_{12}C_{21}P_1P_2 \quad (12)$$

$$B = C_{12}C_{21} - C_{11}C_{22}. \quad (13)$$

In this paper, the sensitivity function is defined as sensitivity of the transfer function $\boldsymbol{G}_{yf}$ from the external force f to the output y with respect to parameter variation of the controlled plant P. These sensitivity functions are given as follows:

$$S_{11} = \frac{\partial \boldsymbol{G}_{yf}(s)_{[1,1]}}{\partial P_1} \frac{P_1}{\boldsymbol{G}_{yf}(s)_{[1,1]}} = \frac{1 + C_{22}P_2}{A} \quad (14)$$

$$S_{22} = \frac{\partial \boldsymbol{G}_{yf}(s)_{[2,2]}}{\partial P_2} \frac{P_2}{\boldsymbol{G}_{yf}(s)_{[2,2]}} = \frac{1 + C_{11}P_1}{A} \quad (15)$$

where $\boldsymbol{G}_{yf}(s)_{[1,1]}$ and $\boldsymbol{G}_{yf}(s)_{[2,2]}$ are the transfer functions from f_1 to y_1 and from f_2 to y_2, respectively.

Then, the complementary sensitivity function Q is defined accordingly as

$$Q_{11} = 1 - S_{11} = (A - 1 - C_{22}P_2)/A \quad (16)$$

$$Q_{22} = 1 - S_{22} = (A - 1 - C_{11}P_1)/A. \quad (17)$$

In addition, we define other parameters Q_{12} and Q_{21} such that they represent the transfer functions from ξ_2 to y_1 and from ξ_1 to y_2 as

$$Q_{12} = C_{21}P_1/A \quad (18)$$

$$Q_{21} = C_{12}P_2/A. \quad (19)$$

As a result, Q_{11}, Q_{12}, Q_{21}, and Q_{22} correspond to transfer functions from (ξ_1, ξ_2) to (y_1, y_2), i.e., noise suppression characteristics. By using parameters Q_{11}, Q_{12}, Q_{21}, and Q_{22}, (5) can be rewritten as follows:

$$\begin{bmatrix} y_1 \\ y_2 \\ u_1 \\ u_2 \end{bmatrix} = \begin{bmatrix} (1 - Q_{11})P_1 & Q_{12}P_2 & -Q_{11} & Q_{12} \\ Q_{21}P_1 & (1 - Q_{22})P_2 & Q_{21} & -Q_{22} \\ -Q_{11} & \dfrac{Q_{12}P_2}{P_1} & \dfrac{-Q_{11}}{P_1} & \dfrac{Q_{12}}{P_1} \\ \dfrac{Q_{21}P_1}{P_2} & -Q_{22} & \dfrac{Q_{21}}{P_2} & \dfrac{-Q_{22}}{P_2} \end{bmatrix} \begin{bmatrix} f_1 \\ f_2 \\ \xi_1 \\ \xi_2 \end{bmatrix}. \quad (20)$$

By solving (12) and (16)–(19) with respect to the controllers C_{11}, C_{12}, C_{21}, and C_{22}, we have the parameterization of

TABLE I
CONDITIONS THAT Q MUST SATISFY

	Conditions
1	Q_{11}, Q_{12}, Q_{21}, and Q_{22} must be stable and proper rational functions.
2	Relative degrees of Q_{11} are greater than or equal to the relative degree of P_1 and Q_{11} must have all unstable zeros of P_1 including infinity zeros as poles.
3	Relative degrees of Q_{12} are greater than or equal to the relative degree of P_1 and Q_{12} must have all unstable zeros of P_1 including infinity zeros as poles.
4	Relative degrees of Q_{21} are greater than or equal to the relative degree of P_2 and Q_{21} must have all unstable zeros of P_2 including infinity zeros as poles.
5	Relative degrees of Q_{22} are greater than or equal to the relative degree of P_2 and Q_{22} must have all unstable zeros of P_2 including infinity zeros as poles.
6	$1 - Q_{11} - Q_{21}$ must have an unstable pole of P_1 and f_1 as zeros.
7	$1 - Q_{12} - Q_{22}$ must have an unstable pole of P_2 and f_2 as zeros.
8	Q_{11} must have an unstable pole of f_1 as zeros.
9	$1 - (P_2/P_1)Q_{12}$ must have an unstable pole of f_2 as zeros.
10	$1 - (P_1/P_2)Q_{21}$ must have an unstable pole of f_1 as zeros.
11	Q_{22} must have an unstable pole of f_2 as zeros.

controllers as follows:

$$C_{11} = \frac{1}{P_1} \frac{(1 - Q_{22})Q_{11} + Q_{12}Q_{21}}{(1 - Q_{11})(1 - Q_{22}) - Q_{12}Q_{21}} \quad (21)$$

$$C_{12} = \frac{1}{P_2} \frac{Q_{21}}{(1 - Q_{11})(1 - Q_{22}) - Q_{12}Q_{21}} \quad (22)$$

$$C_{21} = \frac{1}{P_1} \frac{Q_{12}}{(1 - Q_{11})(1 - Q_{22}) - Q_{12}Q_{21}} \quad (23)$$

$$C_{22} = \frac{1}{P_2} \frac{(1 - Q_{11})Q_{22} + Q_{12}Q_{21}}{(1 - Q_{11})(1 - Q_{22}) - Q_{12}Q_{21}}. \quad (24)$$

From these equations, the controllers are parameterized by the complementary sensitivity functions Q_{11}, Q_{12}, Q_{21}, and Q_{22}. Therefore, it is possible to change the performance of the controller and guarantee the internal stability of the system by designing the Q parameters through the conditions described in Table I. Thus, from the design of these parameters, we can realize a wide range of control performance in the two-channel bilateral control system.

III. DESIGN OF Q PARAMETERS

A. Criteria for Achieving Bilateral Control

The control target of bilateral control is to synchronize the position between the master and slave systems, satisfying the law of action and reaction in the force applied to the master and slave systems. In other words, the position error between the master and slave systems must be zero, and the master and slave systems should be affected by a force equivalent to the one applied to the other system. These targets are expressed by the

following equations:

$$\text{Position} : \left\{ \lim_{t \to \infty} y_1 - y_2 = 0 \right. \tag{25}$$

$$\text{Force} : \left\{ \begin{array}{l} \lim_{t \to \infty} u_1 - f_2 = 0 \\ \lim_{t \to \infty} u_2 - f_1 = 0. \end{array} \right. \tag{26}$$

For this section, assume that all the controlled plants are almost identical. The total driving force $f_i + u_i$ determines the response of the controlled plant P_i. If the applied force and the driving force of the actuator are equal, it is considered that the law of action and reaction is fulfilled. The conditions in (26) guarantee that the total driving force for the two controlled plants is equal. For example, if actual external force f_1 is applied to the controlled plant P_1, the same amount of force u_2 is applied to the controlled plant P_2 according to (26). They represent a virtual law of action and reaction between the two controlled plants, because these two forces are cancelled.

In order to design a bilateral control system, we consider converting these conditions to equivalent practical conditions. First, (5) can be rewritten as follows:

$$\begin{bmatrix} \boldsymbol{t}(s) \\ \boldsymbol{v}(s) \end{bmatrix} = \begin{bmatrix} \boldsymbol{G}_{tf}(s) & \boldsymbol{G}_{t\xi}(s) \\ \boldsymbol{G}_{vf}(s) & \boldsymbol{G}_{v\xi}(s) \end{bmatrix} \begin{bmatrix} \boldsymbol{f}(s) \\ \boldsymbol{\xi}(s) \end{bmatrix} \tag{27}$$

where

$$\boldsymbol{t}(s) = \begin{bmatrix} y_1 - y_2 \\ u_1 + u_2 \end{bmatrix} \tag{28}$$

$$\boldsymbol{v}(s) = \begin{bmatrix} u_1 - f_2 \\ u_2 - f_1 \end{bmatrix} \tag{29}$$

$$\boldsymbol{G}_{tf}(s) = \begin{bmatrix} (1 - Q_{11} - Q_{21})P_1 & (Q_{12} + Q_{22} - 1)P_2 \\ -Q_{11} + Q_{21}P_1/P_2 & Q_{12}P_2/P_1 - Q_{22} \end{bmatrix} \tag{30}$$

$$\boldsymbol{G}_{t\xi}(s) = \begin{bmatrix} -Q_{11} - Q_{21} & Q_{12} + Q_{22} \\ Q_{11}/P_1 + Q_{21}/P_2 & Q_{12}/P_1 - Q_{22}/P_2 \end{bmatrix} \tag{31}$$

$$\boldsymbol{G}_{vf}(s) = \begin{bmatrix} -Q_{11} & -1 + Q_{12}P_2/P_1 \\ -1 + Q_{21}P_1/P_2 & -Q_{22} \end{bmatrix} \tag{32}$$

$$\boldsymbol{G}_{v\xi}(s) = \begin{bmatrix} -Q_{11}/P_1 & Q_{12}/P_1 \\ Q_{21}/P_2 & -Q_{22}/P_2 \end{bmatrix} \tag{33}$$

where $\boldsymbol{t}(s)$ is defined as a vector of the control target consisting of $y_1 - y_2$ and $u_1 + u_2$, and $\boldsymbol{v}(s)$ is the element of force control target consisting of $u_1 - f_2$ and $u_2 - f_1$.

In (27)–(33), we include uncertainties and disturbance equivalently in the external force f_1 and f_2, following the same concept as DOB. In these equations, we want to make errors from position, $y_1 - y_2$, and force, $u_1 - f_2$ and $u_2 - f_1$, to be almost zero if this disturbance exists. In order to achieve this, we select transfer functions from f to each of these errors to be small enough in the following frequency domains: $\boldsymbol{G}_{tf}(s)_{[1,1]}$, $\boldsymbol{G}_{tf}(s)_{[1,2]}$, and $\boldsymbol{G}_{vf}(s)$ are designed to be zero or very small in low-frequency domain. $\boldsymbol{G}_{t\xi}(s)_{[1,1]}$, $\boldsymbol{G}_{t\xi}(s)_{[1,2]}$, and $\boldsymbol{G}_{v\xi}(s)$

are designed to be zero or very small in high-frequency domain, as noise typically contains high-frequency components.

B. Conditions for Q Parameters

Note that characteristics Q_{11}, Q_{12}, Q_{21}, and Q_{22} are related to the following items:
  1) relative degree involved in the controller design;
  2) internal stability of the control system;
  3) control target for the position;
  4) control target for the force.

We have to select these parameters considering the aforementioned items.

The conditions for convergence of $\boldsymbol{t}(s)$ to zero, thus guaranteeing stability of the system, can be found from the transfer functions described in (30)–(33) and they are summarized in Table I. In order to guarantee this conditions, we analyze the transfer functions from (27)–(33); condition 1 is defined through elements $G_{t\xi}(s)_{[1,1]}$, $G_{t\xi}(s)_{[1,2]}$, $G_{vf}(s)_{[1,1]}$, and $G_{vf}(s)_{[2,2]}$, from (31) and (32), this transfer functions represent the position and force error in terms of the noise and external forces. Since we assume that the noises do not have unstable poles, these transfer functions must filter the unstable poles of the external forces. If, for example, the forces are step functions, this means they have an unstable pole at the origin, this unstable pole must be filtered by the designed Q. Condition 2–5 are defined from each of the elements in (33), the plants P_1 and P_2 are considered to have an unstable zeros, and since the plants have a relative degree greater or equal to one in order to be stable and proper, then the plant's transfer function also has a zero at infinity, therefore, to guarantee this conditions, Q should be designed so as to cancel the unstable zeros of P, including infinity. Condition 6 and 7 are defined from the stability condition for transfer functions $G_{tf}(s)_{[1,1]}$ and $G_{tf}(s)_{[1,2]}$ in (30), respectively, since these represent the position error in terms of the external forces and plants, then Q must be design so that $1 - Q_{11} - Q_{21}$ and $Q_{12} + Q_{22} - 1$ cancel the unstable poles of P_1 and P_2 as zeros. Finally, conditions 8–11 are defined in the elements of (32), these transfer functions represent the error for the action–reaction law represented in terms of the external force f_1 and f_2, therefore, the four elements of $G_{vf}(s)$ should suppress the unstable poles of the forces as zeros.

C. Illustrative Example

As an illustrative example, a simple single mass actuator with a damping factor, such as a rotary motor, is considered as a plant model. This model has a single unstable pole at the origin and is given by

$$P_i = \frac{1}{(M_i s + D_i)s} \quad (i = 1, 2) \tag{34}$$

where M_i is inertia of the mover and D_i is the viscous friction coefficient.

External force is assumed as a step function having an unstable zero at the origin. Taking into consideration the conditions in Table I, $1 - Q_{11} - Q_{21}$ must have double zeros at the origin, to satisfy conditions 6 and 7. In addition, from conditions 2–5,
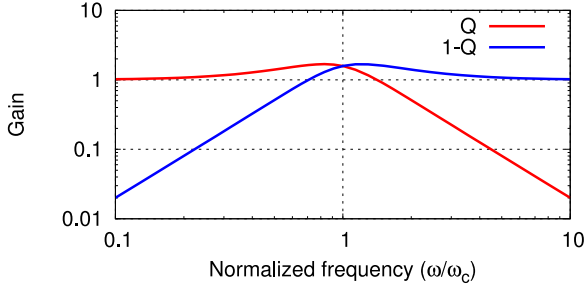
Fig. 2.   Bode plot of Q and $1 - Q$.

the relative degrees of Q_{11} and Q_{12} are equal or less than that of P_1 and the relative degrees of Q_{21} and Q_{22} are equal to or less than that of P_2. Thus, a set of solutions for Q parameters that satisfy the conditions of Table I are as follows:

$$Q_{11} = Q_{22} = 0 \tag{35}$$

$$Q = Q_{12} = Q_{21} = \frac{a_1 s + a_0}{s^3 + a_2 s^2 + a_1 s + a_0} \tag{36}$$

where a_i are coefficients of the Hurwitz polynomial. Fig. 2 shows a Bode plot of $Q = Q_{12} = Q_{21}$.

To summarize, (27) is rewritten as

$$\begin{bmatrix} y_1 - y_2 \\ u_1 + u_2 \\ u_1 - f_2 \\ u_2 - f_1 \end{bmatrix} = \begin{bmatrix} (1-Q)P_1 & -(1-Q)P_2 & -Q & Q \\ \frac{P_1}{P_2}Q & \frac{P_2}{P_1}Q & \frac{Q}{P_2} & \frac{Q}{P_1} \\ 0 & -1 + \frac{P_2}{P_1}Q & 0 & \frac{Q}{P_1} \\ -1 + \frac{P_1}{P_2}Q & 0 & \frac{Q}{P_2} & 0 \end{bmatrix} \begin{bmatrix} f_1 \\ f_2 \\ \xi_1 \\ \xi_2 \end{bmatrix}. \tag{37}$$

We can assume that the external force f_1 and f_2 contain only low-frequency components. On the other hand, the observation noise ξ_1 and ξ_2 contain high-frequency components. The sensitivity function $1 - Q$ is designed as a high-pass filter (HPF), and the complementary sensitivity function Q is designed as a low-pass filter (LPF) in (37). Therefore, $y_1 - y_2$ can converge to zero because it is not affected neither by external force nor observation noise. In the low-frequency domain, $u_1 + u_2$ is almost the same as $f_1 + f_2$ under the assumption $P_1 = P_2$ because it is only affected by external forces. On the other hand, in the high-frequency domain, the observation noise ξ_1 and ξ_2 are suppressed by the LPF. Similarly, u_1 and u_2 can converge to f_2 and f_1, respectively.

We have thus designed the bilateral control using the aforementioned procedure. In the next section, we describe experimental verification of the system. The proposed method can realize high accuracy performance in bilateral control and satisfy the internal stability condition of the control system.

IV. DERIVATION OF REPRODUCIBILITY AND OPERABILITY

The bilateral control system can be represented by a four-terminal circuit model. The relationship between the master–slave position and force is expressed as follows, using a hybrid matrix. In the following expression, X_m is the position of the master, X_s is the position of the slave, F_m is the force applied to the master, and F_s is the force applied to the slave as

$$\begin{bmatrix} F_m \\ X_m \end{bmatrix} = \begin{bmatrix} H_{11} & H_{12} \\ H_{21} & H_{22} \end{bmatrix} \begin{bmatrix} X_s \\ -F_s \end{bmatrix}. \tag{38}$$

Using the aforementioned equation, the relational expression of position and force on the master side is as follows:

$$F_m = \left(\frac{H_{12}}{H_{21} + H_{22}Z_e} Z_e + \frac{H_{11}}{H_{21} + H_{22}Z_e} \right) X_m. \tag{39}$$

We define repeatability P_r and usability P_o as follows:

$$P_r = \frac{H_{12}}{H_{21} + H_{22}Z_e}, P_o = \frac{H_{11}}{H_{21} + H_{22}Z_e}. \tag{40}$$

Here, Z_e is the impedance of the environment contacted on the slave side. Therefore, (39) is rewritten as follows:

$$F_m = (P_o Z_e + P_r) X_m. \tag{41}$$

Reproducibility P_r is an index of reproduction on the master side of environmental impedance Z_e, and operability P_o is an index of the magnitude of the operating force that the operator feels besides the environmental reaction force. The hybrid matrix for ideal reproducibility and operability is expressed as follows:

$$\begin{bmatrix} H_{11} & H_{12} \\ H_{21} & H_{22} \end{bmatrix} = \begin{bmatrix} 0 & 1 \\ 1 & 0 \end{bmatrix}. \tag{42}$$

A. Hybrid Matrix and Reproducibility/Operability in the Proposed Method

The hybrid matrix in the four-terminal circuit of the proposed method shown in Fig. 1 can be expressed as follows:

$$H_{11} = \frac{-P_1(C_{11}(-C_{22}P_2 - 1) + C_{12}C_{21}P_2) + C_{22}P_2 + 1}{C_{12}P_1 P_2} \tag{43}$$

$$H_{12} = \frac{C_{11}P_1 P_2 + P_1}{C_{12}P_1 P_2}, H_{21} = \frac{C_{22}P_2 + 1}{C_{12}P_1 P_2}, H_{22} = \frac{1}{C_{12}}. \tag{44}$$

The four controllers C_{11}–C_{22} are designed to satisfy the control target of expressions (25) and (26). The results of four-channel bilateral control are analyzed using conditions and control systems identical with those of Shimono *et al.* [31] and Mizoguchi *et al.* [32]. Fig. 3 shows a frequency characteristic when $Z_e = 30 + 5s$ is used as a relatively soft environment. Fig. 3 is discussed in Section VII-B.

V. REDESIGN OF COMPLEMENTARY SENSITIVITY FUNCTION

In Section III, we had set Q_{11}, $Q_{22} = 0$, Q_{12}, $Q_{21} = $ LPF for the four complementary sensitivity functions. In this section, these four complementary sensitivity functions are further examined and different designs are described.

Table I, which shows the conditions to be satisfied by the complementary sensitivity function, lists three types of conditions. First, the conditions 2–5 make sure the transfer function of the controller is appropriate. Second, there are conditions that satisfy the internal stability of the entire control system. Third, conditions 2–5 include functions to achieve the control target of bilateral control.
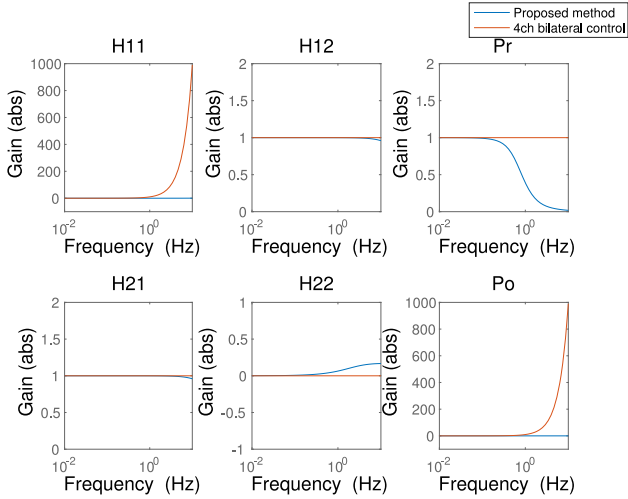
Fig. 3. Analysis result of reproducibility, operability, and hybrid matrix.

Fig. 4. Equivalent circuit of the proposed method in the case of using the HPF.

We redesign the complementary sensitivity functions to satisfy the aforementioned conditions as follows:

$$Q_{11} = Q_{22}$$
$$= \text{HPF} = Q_{\text{HPF}} = \frac{s^3 + a_2 s^2}{s^3 + a_2 s^2 + a_1 s + a_0} \quad (45)$$
$$Q_{12} = Q_{21}$$
$$= \text{LPF} = Q_{\text{LPF}} = \frac{a_1 s + a_0}{s^3 + a_2 s^2 + a_1 s + a_0} \quad (46)$$
$$Q_{\text{HPF}} + Q_{\text{LPF}} = 1. \quad (47)$$

Q_{11} and Q_{22} are HPFs with third-order Butterworth coefficients, and Q_{12} and Q_{21} are LPFs. The frequency characteristics of this filters are shown in Fig. 2. By designing the Q parameter as described previously, it is possible to relax the condition of the control target regarding to the position. This is because $1 - Q_{11} - Q_{21}$, $(Q_{12} + Q_{22}) - 1$ become 0 in (30). In other words, conditions 2–5 represent a function in which the relative degree of the complementary sensitivity function Q_{11}, Q_{22} is 2 or more, and the complementary sensitivity function Q_{12}, Q_{21} has one or more zeros.

In this case, the controller transfer function is as follows:

$$C_{\text{one}} = C_{11} = C_{12} = C_{21} = C_{22} = \frac{Q_{12}}{PQ_{11}} = \frac{1}{P} \frac{a_1 s + a_0}{s^3 + a_2 s^2}. \quad (48)$$

The four controllers are identical, and the dimension of the controller transfer function can be reduced.

Since the four controllers in the proposed method are identical, the configuration of the control system can be simplified. In the bloc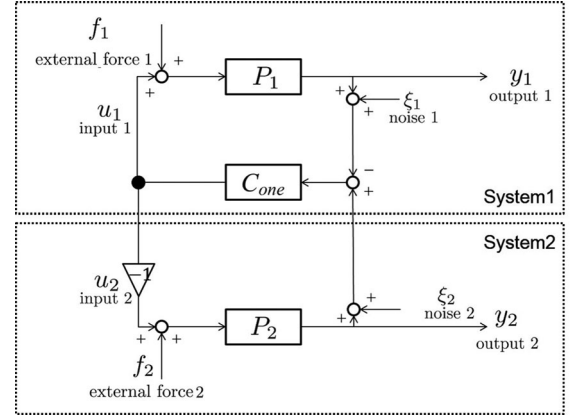k diagram of the original method, a controller derived for each master/slave system is required. However, as the command value to the master/slave system is the output of the same controller with a different sign of the input signal, the block diagram can be simplified to Fig. 4. Haptic transmission technology can be realized using a single controller by changing the complementary sensitivity function. The transfer function of the control system as a whole becomes (49), shown at the bottom of this page, where the transfer function of external force f_1, f_2 to $y_1 - y_2$ is 0, and the transfer function of observation noise ξ_1, ξ_2 is 1. Therefore, $y_1 - y_2$ can theoretically converge to 0 without being influenced by external forces, however, it is expected to be affected by the observed noise. Similarly, the transfer function of external force f_1 to u_1 is HPF and the transfer function of external force f_2 to u_1 is LPF. The transfer function of observation noise ξ_1, ξ_2 to u_1 is LPF; therefore, u_1 converges to f_2 because it is affected only by external force f_2. Similarly, u_2 can converge to f_1. The sum of the outputs of the controller $u_1 + u_2$ converges to $f_1 + f_2$, and $u_1 + u_2$ becomes 0 from the controller design. It is possible to satisfy the law of action and reaction in external force f_1, f_2 and realize haptic transmission technology.

VI. INTRODUCTION OF MICRO/MACRO BILATERAL CONTROL

Micro/macro bilateral control seeks to change the position/force ratio in the master/slave system to an arbitrary value. We change the control target of the bilateral control system to change the scaling ratio between the master and the slave. The control target of the micro/macro bilateral control is as follows:

$$\text{Position} = \{ \lim_{t \to \infty} \alpha_p y_1 - \beta_p y_2 = 0 \quad (50)$$

$$\text{Force} = \begin{cases} \lim_{t \to \infty} \beta_f u_1 - f_2 = 0 \\ \lim_{t \to \infty} \alpha_f u_2 - f_1 = 0. \end{cases} \quad (51)$$

$$\begin{bmatrix} y_1 - y_2 \\ u_1 + u_2 \\ u_1 \\ u_2 \end{bmatrix} = \begin{bmatrix} 0 & 0 & 1 & 1 \\ -Q_{\text{HPF}} + \frac{P_1}{P_2}Q_{\text{LPF}} & \frac{P_2}{P_1}Q_{\text{LPF}} - Q_{\text{HPF}} & -\frac{Q_{\text{HPF}}}{P_1} + \frac{Q_{\text{LPF}}}{P_2} & \frac{Q_{\text{LPF}}}{P_1} - \frac{Q_{\text{HPF}}}{P_2} \\ -Q_{\text{HPF}} & \frac{P_2}{P_1}Q_{\text{LPF}} & -\frac{Q_{\text{HPF}}}{P_1} & \frac{Q_{\text{LPF}}}{P_1} \\ \frac{P_1}{P_2}Q_{\text{LPF}} & -Q_{\text{HPF}} & \frac{Q_{\text{LPF}}}{P_2} & -\frac{Q_{\text{HPF}}}{P_2} \end{bmatrix} \begin{bmatrix} f_1 \\ f_2 \\ \xi_1 \xi_2 \end{bmatrix} \quad (49)$$

Here, α_p, α_f and β_p, β_f are scaling factors. In these control target equations, scaling factors for position α_p, β_p and for force α_f, β_f are used so that the position and force scaling ratio between the master and the slave can be changed independently. The transfer function of the whole system in the case of micro/macro bilateral control is expressed as follows:
It is possible to design the system in the same way as bilateral control by determining the Q parameter as follows, with (52) shown at the bottom of this page:

$$Q_{11} = Q_{22} = 0 \tag{53}$$

$$Q_{12} = \beta_f Q \tag{54}$$

$$Q_{21} = \alpha_f Q \tag{55}$$

$$Q = \frac{a_1 s + a_0}{s^3 + a_2 s^2 + a_1 s + a_0}. \tag{56}$$

After designing the complementary sensitivity function, the controller of the proposed method with the introduction of micro/macro bilateral control can be determined as follows:

$$C_{\text{scale}11} = \frac{1}{P_1} \frac{\alpha_f \beta_f Q^2}{1 - \alpha_f \beta_f Q^2} \tag{57}$$

$$C_{\text{scale}12} = \frac{1}{P_2} \frac{\alpha_f Q}{1 - \alpha_f \beta_f Q^2} \tag{58}$$

$$C_{\text{scale}21} = \frac{1}{P_1} \frac{\beta_f Q}{1 - \alpha_f \beta_f Q^2} \tag{59}$$

$$C_{\text{scale}22} = \frac{1}{P_2} \frac{\alpha_f \beta_f Q^2}{1 - \alpha_f \beta_f Q^2}. \tag{60}$$

By expressing the transfer function of the controller using a scaling factor with respect to force, it is possible to change the ratio of the force between the master and the slave. A change in the scaling ratio of the position is also achieved by using the scaling factor for the position information input to the controller. The block diagram of the micro/macro bilateral control for the proposed method is shown in Fig. 5. Since the transfer function of the whole control system and the controller are the same as in the case of bilateral control, the reproducibility and operability for micro/macro bilateral control are the same as for bilateral control.
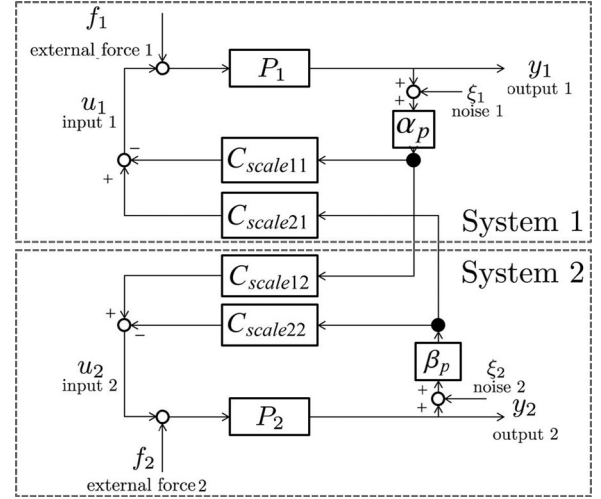

Fig. 5. Block diagram of the proposed bilateral control system with scaling.

VII. EXPERIMENTAL RESULTS

The performance of the proposed control is evaluated experimentally and compared with that of the conventional four-channel bilateral control. Three methods are compared: bilateral control of the proposed method, four-channel bilateral control, and micro/macro bilateral control of the proposed method whose scaling ratio for position is master : slave $= 1 : 5$ and the scaling ratio for force is master : slave $= 1 : 1$.

A. Experimental Configuration

In the experiments, a pair of ac servo motors with end effectors are utilized as controlled plants. Human force f_{man} is imposed in the master system, and reaction force from environment is applied to the slave system when its end effector interacts with the environment. The parameters of the control system are as shown in Table II. Where the inertia of the plant model and sampling time are obtained from the manufacturer specifications of the plant model and sampling time are obtained from the manufacturer specifications of the plant and encoder, the viscous friction was estimated using identification methods, the coefficients of the third-order filter have been selected from the general formula for the third-order Butterworth filter, while

$$\begin{bmatrix} \alpha_p y_1 - \beta_p y_2 \\ \beta_f u_1 + \alpha_f u_2 \\ \beta_f u_1 - f_2 \\ \alpha_f u_2 - f_1 \end{bmatrix} = \begin{bmatrix} \alpha_p \left(1 - \frac{\beta_p}{\alpha_p} Q_{21}\right) P_1 & -\beta_p \left(1 - \frac{\alpha_p}{\beta_p} Q_{12}\right) P_2 & -\beta_p Q_{21} & \alpha_p Q_{12} \\ \alpha_f \frac{P_1}{P_2} Q_{21} & \beta_f \frac{P_2}{P_1} Q_{12} & \beta_f \frac{Q_{21}}{P_2} & \alpha_f \frac{Q_{12}}{P_1} \\ 0 & -1 + \beta_f \frac{P_2}{P_1} Q_{12} & 0 & \beta_f \frac{Q_{12}}{P_1} \\ -1 + \alpha_f \frac{P_1}{P_2} Q_{21} & 0 & \alpha_f \frac{Q_{21}}{P_2} & 0 \end{bmatrix} \begin{bmatrix} f_1 \\ f_2 \\ \xi_1 \\ \xi_2 \end{bmatrix} \tag{52}$$

TABLE II
PARAMETERS OF SIMULATION AND EXPERIMENT

| Parameters	Meaning	Values
M_1	Inertia of plant model 1	0.40×10^{-4} [kg· m^2]
M_2	Inertia of plant model 2	0.40×10^{-4} [kg·m^2]
D_1	Viscous friction of plant model 1	6.375×10^{-4} [N·m/rad/s]
D_2	Viscous friction of plant model 2	6.375×10^{-4} [N·m/rad/s]
ω_c	Cutoff frequency in controller	340 [rad/s]
ω_{LPF}	Cutoff frequency in LPF	500[rad/s]
a_0	Coefficient of third-order filter	ω_c^3
a_1	Coefficient of third-order filter	$2\omega_c^2$
a_2	Coefficient of third-order filter	$2\omega_c$
ω_{DOB}	Cut-off frequency in DOB	500[rad/s]
K_P	Position gain	7000
K_V	Velocity gain	350
K_f	Force gain	1
α_p	Scaling gain for position	1.0
β_p	Scaling gain for position	0.2
α_f	Scaling gain for force	1.0
β_f	Scaling gain for force	1.0
	Sampling time	50 [μs]
	Resolution precision of the rotary encoder	20 [bit]
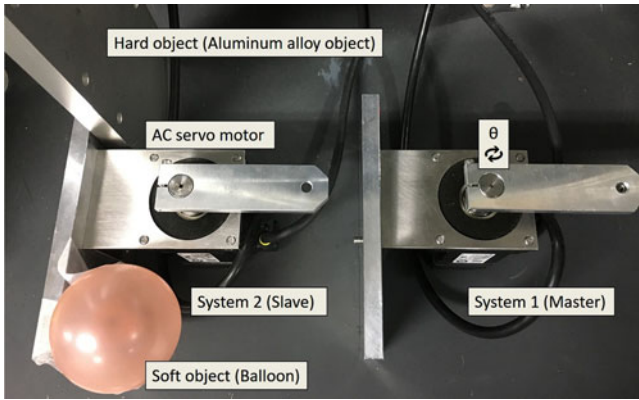
Fig. 6. Experimental units with hard and soft objects.

the cutoff frequencies have been selected by adjusting them to the characteristics of the system. The control gain is raised to the point just before vibration due to noise occurs in each control method and the scaling gain is defined according to the ratios defined in the experiment (1:5 and 1:1 for position and force, respectively). The experimental setup is shown in Fig. 6. In these experiments, a soft object (balloon) and a hard object (A5052 aluminium alloy object) are used as manipulated objects. Here, response of a human and reaction force are estimated by a reaction force observer, but they are not used in the proposed control system. $\hat{f}_{\mathrm{man}}$ and $\hat{f}_{\mathrm{exp}}$ are the estimated human force and the reaction force. Fig. 7 shows experimental results in soft and hard environments.

B. Discussion

Here, we will describe the experimental results and transparency/stability analysis results.

Experimental results for bilateral control are shown in Fig. 7(a), (b), (d), and (e), where Fig. 7(a) and (d) shows results for the proposed, two-channel bilateral control, method

and Fig. 7(b) and (e) shows the results for the conventional, four-channel bilateral control.

From the plots of position and position error, it can be seen that the position of the slave system follows that of the master system. The position error arises only when the acceleration is large, and it is essentially zero when the master is stationary. The cause of the error is the cutoff frequency ω_c not being sufficiently high, and the nominal error of inertia. Regarding the force response, the estimated human force $\hat{f}_{\mathrm{man}}$ and the input of the slave system u_2, as well as the estimated reaction force from soft environment $\hat{f}_{\mathrm{ext}}$ and the input of the master system u_1 are almost synchronized. This proves that the operator can feel the reaction force from the environment with a small error. It can also be seen that the sum of action and reaction force, $\hat{f}_{\mathrm{man}} + \hat{f}_{\mathrm{ext}}$, is almost zero, i.e., the control system satisfies the law of action and reaction.

Experimental results for the micro/macro bilateral control of the proposed method are shown in Fig. 7(c) and (f). The scaling ratio for position is master : slave $= 1 : 5$ and that for force is master : slave $= 1 : 1$. In other words, the position response of the slave side is five times larger than that of the master side, and the same force is transmitted to both the master side and the slave side. The results for micro/macro bilateral control are similar to those of bilateral control. However, the accuracy of the response with respect to the position where the scaling ratio is being changed shows deterioration. It is seen that error occurs in the position between the master and the slave when the slave is in contact with the environment. The error has occurred in multiples with respect to the scaling ratio. We consider the error to be caused by differences in encoder resolution between the master and the slave. Therefore, we must solve this problem in the future.

Root mean squares of these errors are summarized in Table III. Four-channel bilateral control performs friction compensation by reaction force estimation observer, but the proposed method adds the identified frictional force to the command value. Friction compensation is performed when the operation velocity exceeds a certain value and is not performed when it does not exceed that value. The sum of force estimates is disturbed when switching friction compensation. Therefore, the mean square error of force is larger for the proposed method. This is inferred from the results for micro/macro bilateral control in which the operation velocity is increased.

From analyzing the results in Fig. 3(a) and (c), in four-channel bilateral control, the elements of the hybrid matrix H_{11} and operability P_o are far from the ideal value in the high-frequency range. In the proposed method, the hybrid matrix is almost ideal, but the reproducibility P_r is close to 0 in the high-frequency range. Therefore, the proposed method, which is two-channel bilateral control, emphasizes operability, while the four-channel bilateral control emphasizes reproducibility. This difference is considered to be caused by the difference in the control considered important in bilateral control—Position control or force control. This is clearly shown in the experimental results. Emphasis on reproducibility as in four-channel bilateral control leads to improved transmission of force between the master and the slave. Conversely, if emphasis is placed on operability as in
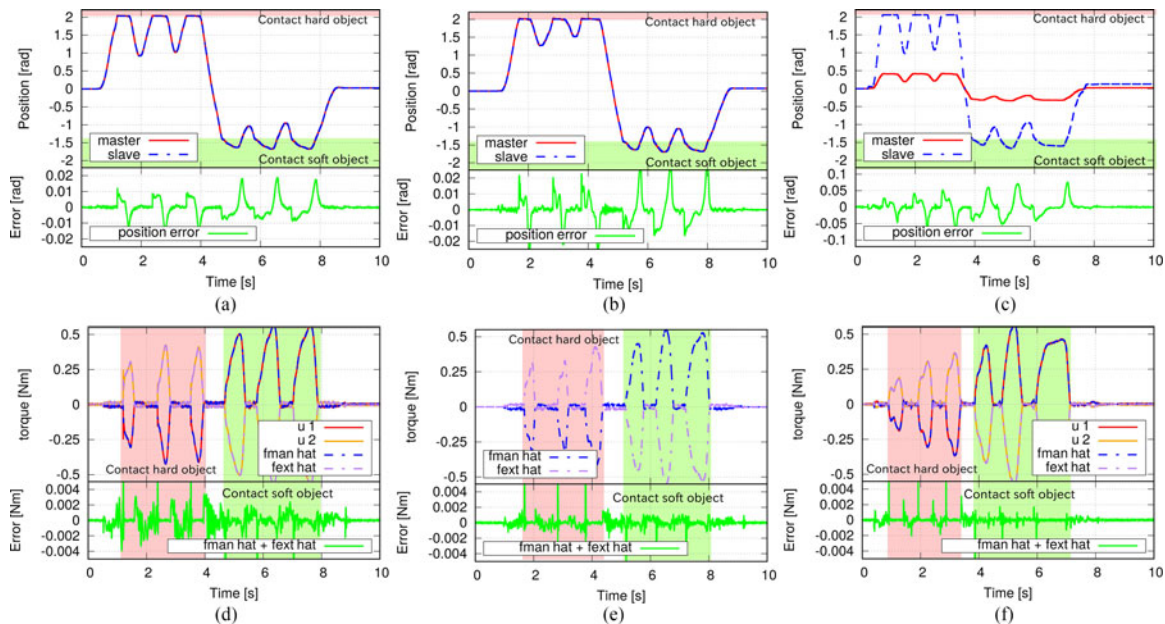
Fig. 7. Experimental results of the proposed method and four-channel bilateral control. (a) Position results in the proposed method without scaling. (b) Position results in four-channel architecture bilateral control. (c) Position results in the proposed method with scaling ($m{:}s = 1{:}5$). (d) Force results in the proposed method without scaling. (e) Force results in four-channel architecture bilateral control. (f) Force results in the proposed method with scaling ($m{:}s = 1{:}1$).

TABLE III
ROOT MEAN SQUARE OF ERROR

Condition	Index	Value
Bilateral control	position [rad]	0.005035
of the proposed method	force [mN.m]	1.38
Bilateral control	position [rad]	0.00737
of 4ch architecture	force [mN.m]	0.72
Micro/macro bilateral control	position [rad]	1.03425
of the proposed method	force [mN.m]	0.46

the proposed method, position tracking between the master and the slave is improved.

VIII. CONCLUSION

In this paper, a transfer-function-based approach for designing bilateral control systems is presented. The controller is parametrized by the complementary sensitivity function Q, which is determined from the conditions derived from internal stability of the system and convergence criteria of the control target of the bilateral system. Through experiments, we confirmed that the proposed control realizes higher performance and requires fewer communication channels than the conventional four-channel bilateral control both in soft and hard environments. For future work, we will investigate an environment with multiple degrees of freedom and extend the system to multilateral control.

REFERENCES

[1] K. Ohnishi, S. Katsura, and T. Shimono, "Motion control for real-world haptics," *IEEE Ind. Electron. Mag.*, vol. 4, no. 2, pp. 16–19, Jun. 2010, doi: 10.1109/MIE.2010.936761.

[2] C. D. Onal, "Bilateral control a sliding mode control approach," Master's thesis, Sabanci University, Istanbul, Turkey, 2005.

[3] T. Shimono, S. Katsura, and K. Ohnishi, "Abstraction and reproduction of force sensation from real environment by bilateral control," *IEEE Trans. Ind. Electron*, vol. 54, no. 2, pp. 907–918, Mar. 2007, doi: 10.1109/TIE.2007.892744.

[4] Y. Matsumoto, S. Katsura, and K. Ohnishi, "An analysis and design of bilateral control based on disturbance observer," in *Proc. IEEE Int. Conf. Ind. Technol.*, May. 2003, pp. 802–807, doi: 10.1109/ICIT.2003.1290760.

[5] S. Katsura, Y. Matsumoto, and K. Ohnishi, "Realization of law of action and reaction by multilateral control," *IEEE Trans. Ind. Electron*, vol. 52, no. 5, pp. 1196–1205, Sep. 2005, doi: 10.1109/TIE.2005.855699.

[6] B. Hannaford, "A design framework for teleoperators with kinesthetic feedback," *IEEE Trans. Robot. Autom.*, vol. 5, no. 4, pp. 426–434, Aug. 1989, doi: 10.1109/70.88057.

[7] D. A. Lawrance, "Stability and transparency in bilateral teleoperation," *IEEE Trans. Robot. Autom.*, vol. 9, no. 5, pp. 624–637, Oct. 1993, doi: 10.1109/70.258054.

[8] J. Li, M. Tavakoli, and Q. Huang, "Absolute stability of multi-DOF multilateral haptic systems," *IEEE Trans. Control Syst. Technol.*, vol. 22, no. 6, pp. 2319–2328, Nov. 2014, doi: 10.1109/TCST.2014.2301840.

[9] A. Sabanovic and K. Ohnishi, *Motion Control Systems (ser. 10)*, vol. 4. Singapore: Wiley, 2011.

[10] Y. Yokokohji and T. Yoshikawa, "Bilateral control of master-slave manipulators for ideal kinesthetic coupling-formulation and experiment," *IEEE Trans. Robot. Autom.*, vol. 10, no. 5, pp. 605–620, Oct. 1994, doi: 10.1109/70.326566.

[11] K. Hashtrudi-Zaad and S. E. Salcudean, "Bilateral parallel force/position teleoperation control," *J. Robot. Syst.*, vol. 19, no. 4, pp. 155–167, Mar. 2002, doi: 10.1002/rob.10030.

[12] K. Hashtrudi-Zaad and S. E. Salcudean, "Transparency in time-delayed systems and the effect of local force feedback for transparent teleoperation," *IEEE Trans. Robot. Autom.*, vol. 18, no. 1, pp. 108–114, Aug. 2002, doi: 10.1109/70.988981.

[13] S. Katsura, W. Iida, and K. Ohnishi, "Medical mechatronics an application to haptic forceps," *Annu. Rev. Control*, vol. 29, no. 2, pp. 237–245, 2005.

[14] T. Takei, T. Shimono, and K. Ohnishi, "Dynamic estimation of environmental stiffness by bilateral control," *IEEJ Trans. Ind. Appl.*, vol. 129, no. 6, pp. 601–607, 2009, doi: 10.1541/ieejias.129.601.

[15] T. Shimono, S. Katsura, S. Susa, T. Takei, and K. Ohnishi, "Transmission of real world force sensation by micro/macro bilateral control based on acceleration control with standardization matrix," *IEEJ Trans. Ind. Appl.*, vol. 128, no. 6, pp. 726–732, 2008, doi: 10.1541/ieejias.128.726.

[16] A. Sabanovic, M. Elitas, and K. Ohnishi, "Sliding modes in constrained systems control," *IEEE Trans. Ind. Electron.*, vol. 55, no. 9, pp. 3332–3339, Sep. 2008, doi: 10.1109/TIE.2008.928112.

[17] B. K. Kim, W. K. Chung, and K. Ohba, "Design and performance tuning of sliding-mode controller for high-speed and high-accuracy positioning systems in disturbance observer framework," *IEEE Trans. Ind. Electron.*, vol. 56, no. 10, pp. 3798–3809, Oct. 2009, doi: 10.1109/TIE.2009.2028357.

[18] S. Khan, A. Sabanovic, and A. O. Nergiz, "Scaled bilateral teleoperation using discrete-time sliding-mode controller," *IEEE Trans. Ind. Electron.*, vol. 56, no. 9, pp. 3609–3618, Sep. 2009, doi: 10.1109/TIE.2009.2018538.

[19] S. Sakaino, T. Sato, and K. Ohnishi, "Precise position/force hybrid control with modal mass decoupling and bilateral communication between different structures," *IEEE Trans. Ind. Informat.*, vol. 7, no. 2, pp. 266–276, May 2011, doi: 10.1109/TII.2011.2121077.

[20] M. Takeya, Y. Kawamura, and S. Katsura, "Data reduction design based on delta-sigma modulator in quantized scaling-bilateral control for realizing of haptic broadcasting," *IEEE Trans. Ind. Electron.*, vol. 63, no. 3, pp. 1962–1971, Mar. 2016, doi: 10.1109/TIE.2015.2512233.

[21] E. A. Baran, A. Kuzu, S. Bogosyan, M. Gokasan, and A. Sabanovic, "Comparative analysis of a selected DCT-based compression scheme for haptic data transmission," *IEEE Trans. Ind. Informat.*, vol. 12, no. 3, pp. 1146–1155, Jun. 2016, doi: 10.1109/TII.2016.2555982.

[22] M. Tajiri and Y. Fujimoto, "Bilateral control without force estimation," in *Proc. IEEJ Int. Workshop Sens., Actuation, Motion Control, Optimization*, 2015, vol. 9.

[23] M. Tajiri and Y. Fujimoto, "Design of bilateral control based on complementary sensitivity function using velocity information," in *Proc. Ind. Electron. Conf.*, 2015, pp. 4412–4417.

[24] S. Katsura and K. Ohnishi, "A realization of haptic training system by multilateral control," *IEEE Trans. Ind. Electron.*, vol. 53, no. 6, pp. 1935–1942, Dec. 2006, doi: 10.1109/TIE.2006.885465.

[25] H. Tanaka *et al.*, "Implementation of bilateral control system based on acceleration control using FPGA for multi-DOF haptic endoscopic surgery robot," *IEEE Trans. Ind. Electron.*, vol. 56, no. 3, pp. 618–627, Mar. 2009.

[26] K. Miura, A. Matsui, and S. Katsura, "High-stiff motion reproduction using position-based motion-copying system with acceleration-based bilateral control," *IEEE Trans. Ind. Electron.*, vol. 62, no. 12, pp. 7631–7642, Dec. 2015, doi: 10.1109/TIE.2015.2458957.

[27] S. Yajima and S. Katsura, "Multi-DOF motion reproduction using motion-copying system with velocity constraint," *IEEE Trans. Ind. Electron.*, vol. 61, no. 7, pp. 3765–3775, Jul. 2014, doi: 10.1109/TIE.2013.2286086.

[28] Z. MA and P. Ben-Tzvi, "RML glove: An exoskeleton glove mechanism with haptics feedback," *IEEE/ASME Trans. Mechatronics*, vol. 20, no. 2, pp. 641–652, Apr. 2015.

[29] R. Kubo, T. Shimono, and K. Ohnishi, "Flexible controller design of bilateral grasping systems based on a multilateral control scheme," *IEEE Trans. Ind. Electron.*, vol. 56, no. 1, pp. 62–68, Jan. 2009, doi: 10.1109/TIE.2008.2007010.

[30] D. Prattichizzo, F. Chinello, C. Pacchierotti, and M. Malvezzi, "Towards wearability in fingertip haptics: A 3-DOF wearable device for cutaneous force feedback," *IEEE Trans. Haptics*, vol. 6, no. 4, pp. 506–516, Oct. 2013, doi: 10.1109/TOH.2013.53.

[31] T. Shimono, S. Katsura, S. Susa, T. Takei, and K. Ohnishi, "Transmission of force sensation by micro-macro bilateral control with respect to standardized modal space," in *Proc. IEEE Int. Conf. Mechatronics*, May 2007, pp. 1–6, doi: 10.1109/ICMECH.2007.4280061.

[32] T. Mizoguchi, T. Nozaki, and K. Ohnishi, "Stiffness transmission of scaling bilateral control system by gyrator element integration," *IEEE Trans. Ind. Electron.*, vol. 61, no. 2, pp. 1033–1043, Feb. 2014, doi: 10.1109/TIE.2013.2264787.

[33] S. Sakaino, T. Sato, and K. Ohnishi, "Multi-DOF micro-macro bilateral controller using oblique coordinate control," *IEEE Trans. Ind. Informat.*, vol. 7, no. 3, pp. 446–454, Aug. 2011, doi: 10.1109/TII.2011.2158837.

Masahiro Tajiri (S'15) received the B.E. and M.E. degrees in electrical and computer engineering from Yokohama National University, Yokohama, Japan, in 2015 and 2017, respectively.

He is currently working as a Designer and Developer in the automotive supplier industry. His research interests include haptics and motion control.

Pablo López received the B.E. degree in computer and systems from the University of San Carlos of Guatemala, Guatemala City, Guatemala, in 2014. He is currently working toward the M.E. degree in electrical and computer engineering at Yokohama National University, Yokohama, Japan.

His research interests include motion control.

Yasutaka Fujimoto (S'93–M'98–SM'12) received the B.E., M.E., and Ph.D. degrees in electrical and computer engineering from Yokohama National University, Yokohama, Japan, in 1993, 1995, and 1998, respectively.

In 1998, he joined Keio University, Yokohama. Since 1999, he has been with the Faculty of Engineering, Yokohama National University, where he is currently a Professor. His research interests include actuators, robotics, manufacturing automation, and motion control.

Dr. Fujimoto is an Associate Editor for the IEEE TRANSACTIONS ON INDUSTRIAL ELECTRONICS and *IEEJ Journal of Industry Applications*.